

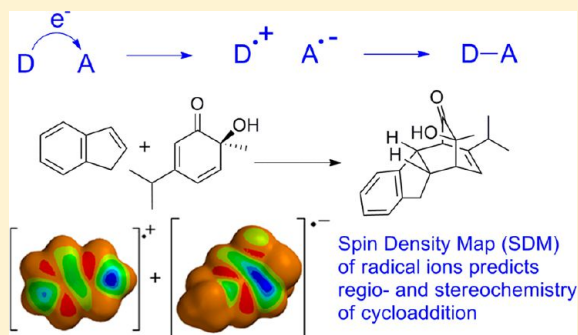
# Beyond Frontier Molecular Orbital Theory: A Systematic Electron Transfer Model (ETM) for Polar Bimolecular Organic Reactions

Katharine J. Cahill and Richard P. Johnson\*

Department of Chemistry, University of New Hampshire, Durham, New Hampshire 03824, United States

**S** Supporting Information

**ABSTRACT:** Polar bimolecular reactions often begin as charge-transfer complexes and may proceed with a high degree of electron transfer character. Frontier molecular orbital (FMO) theory is predicated in part on this concept. We have developed an electron transfer model (ETM) in which we *systematically* transfer one electron between reactants and then use density functional methods to model the resultant radical or radical ion intermediates. Sites of higher reactivity are revealed by a composite spin density map (SDM) of odd electron character on the electron density surface, assuming that a new two-electron bond would occur preferentially at these sites. ETM correctly predicts regio- and stereoselectivity for a broad array of reactions, including Diels–Alder, dipolar and ketene cycloadditions, Birch reduction, many types of nucleophilic additions, and electrophilic addition to aromatic rings and polyenes. Conformational analysis of radical ions is often necessary to predict reaction stereochemistry. The electronic and geometric changes due to one-electron oxidation or reduction parallel the reaction coordinate for electrophilic or nucleophilic addition, respectively. The effect is more dramatic for one-electron reduction.



## INTRODUCTION

The prediction of regio- and stereoselectivity in bimolecular organic reactions remains a broad challenge for modern theoretical methods.<sup>1–3</sup> Intense efforts under way to design enantioselective and catalytic reactions rely on fundamental principles of regio- and diastereoselection.<sup>4</sup> Geometric distortion in transition states is of fundamental importance.<sup>5</sup> During the past four decades, frontier molecular orbital (FMO) theory, originally advanced by Fukui, has played a dominant role as one of the simplest approaches to this important problem.<sup>6</sup> More recently, hard–soft interactions,<sup>7</sup> conceptual DFT,<sup>8</sup> and related theories have been developed and widely applied to define reactivity and selectivity.<sup>3,9</sup> Distortion of orbitals,<sup>10,11</sup> distortion of molecular geometries,<sup>12</sup> and transition state stereoelectronic effects<sup>10,13</sup> have been ascribed important roles in  $\pi$  face diastereoselectivity. This is an enormous field of scientific endeavor in need of additional unifying principles.

We explore here a general method that builds on the concepts of FMO, charge-transfer, and Marcus theories, is operationally simple with modern computational methods, and may provide insight into diverse reaction mechanisms.

## RESULTS AND DISCUSSION

**A Systematic Electron Transfer Model.** The conceptual basis for our approach is illustrated in Figure 1 for the case for two neutral reactants. In the reaction between a donor (D) and acceptor (A), initial formation of a charge transfer complex<sup>14</sup> can lead to product D–A through a continuum of potential

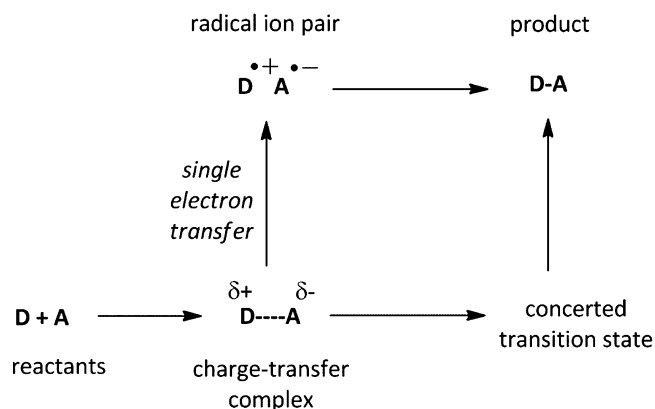


**Figure 1.** Continuum of polarized bimolecular reaction mechanisms.

mechanisms, ranging from polar concerted (horizontal axis) to single electron transfer (vertical axis). The potential complexity of this initial charge-transfer interaction has recently been demonstrated by Rosokha and Kochi.<sup>15</sup> Most polar organic chemical reactions presumably follow a path somewhere in the broad middle of this continuum, far removed from reactants and with a significant degree of electron transfer along the reaction coordinate.

**Special Issue:** Howard Zimmerman Memorial Issue

**Received:** August 14, 2012

**Published:** October 11, 2012

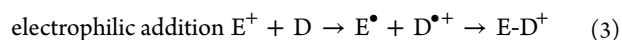
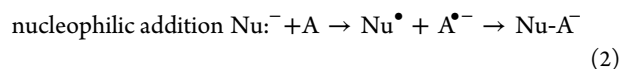
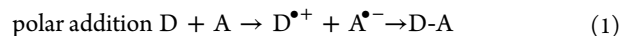
According to the language of Mulliken charge-transfer theory,<sup>14</sup> the transition state (activated complex) will be stabilized by partial electron transfer from donor HOMO to acceptor LUMO. This is commonly described by FMO methods, which capture polarization of reactants through examination of preferred HOMO–LUMO interactions, attempting to pair up the more reactive sites by orbital coefficients or other indicators and to rationalize reactivity through HOMO–LUMO energy differences.<sup>1</sup> Fukui functions and related methods extract different descriptors of electrophilic or nucleophilic sites from the electronic structure of reactants.<sup>9c,16</sup>

A stepwise process that proceeds by complete electron transfer to yield radical ions (Figure 1, vertical axis) lies at the extreme of this polarization continuum. Many organic reactions are known or have been conjectured to proceed by initial electron transfer.<sup>17</sup> Marcus theory<sup>18</sup> has been widely applied to understand the rates of electron transfer and their relationship to reaction energetics.<sup>17a</sup> An implicit flaw in FMO<sup>17e</sup> and related methods is the focus on reactants rather than transition states or intermediates, with the consequent underestimation of polarization and neglect of changes in geometry.<sup>19</sup> In the present study, we sought to develop a general computational model that projects beyond the FMO stage of reaction. Building on FMO and charge-transfer concepts, we choose to *systematically* project along the single electron transfer coordinate to the stage of radicals or radical ions. *Every* polar reaction is thus treated as beginning with single electron transfer. Our expectation was that the easily calculated electronic properties of radical ions and radicals would reveal preferred sites of reactivity, while their optimized geometries might point toward reaction stereochemistry. We refer to this simple approach as an electron transfer model (ETM). The term “model” is included to emphasize that ETM does *not* presume a radical ion mechanism but rather posits that projection along the electron transfer continuum should follow a reaction coordinate similar to polar covalent reactions. At worst, ETM will be an exaggeration of the degree of electron transfer in a polar reaction; at best, it may provide clearer indicators for selectivity, as well as hints about potential mechanisms. Of course, ETM is not novel conceptually and there is already much known about radical ion structure and chemistry,<sup>20</sup> but our systematic approach and straightforward computational model have not, to our knowledge, been described. We note that proton-coupled electron transfer (PCET), in which electron transfer and protonation are considered simultaneously, has been well explored.<sup>21</sup>

The similarity between covalent and single electron transfer reaction coordinates was noted earlier by Pross and co-workers, who drew a two-dimensional grid similar to Figure 1 and advanced the concept of “single electron shifts”.<sup>22</sup> Pross noted that the S<sub>N</sub>2 and similar polar reactions may best be described as a single electron transfer, rather than the more conventional two electron “curved arrow” mechanism. Shaik and Pross have advanced a valence-bond configuration mixing model which describes changes in charge distribution along a reaction coordinate.<sup>23</sup> Our model explicitly considers the electronic and geometric consequences of single electron transfer. ETM may initially seem counterintuitive, but it is really just projection along a reaction coordinate that maximizes charge transfer and thus clarifies its effects.

Equations 1–3 summarize the three most common types of polar bimolecular reactions. In the ETM description of a polar

addition with two neutral reactants, (eq 1) we transfer an electron in the direction that is more probable based on reactant electronic structures and then match up the indicated sites of bonding in the pair of radical ions. For a nucleophilic addition (eq 2), ETM transfers an electron from the nucleophile to acceptor, resulting in a radical and a radical anion. In this case, the main question will be the reactive site and geometric changes in the acceptor radical anion. For electrophilic additions (eq 3), the donor radical cation should hold the most information.



The energetics of single electron transfer are most commonly described by Marcus theory.<sup>18</sup> The connection between ETM and Marcus theory is evident from Figure 2. An ETM

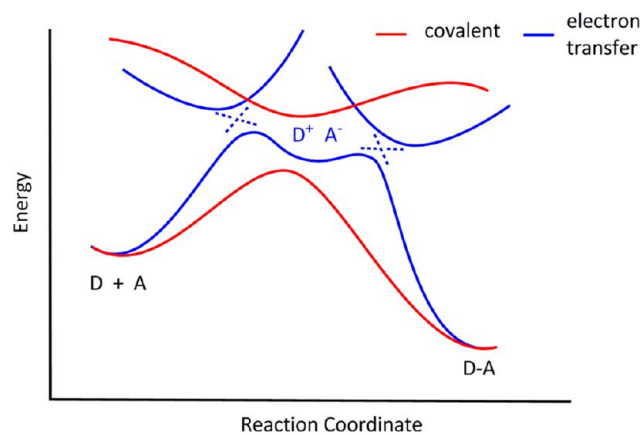


Figure 2. Covalent and electron transfer reaction coordinates.

mechanism would proceed by two steps, both described by a curve crossing. In Figure 2, the covalent reaction curve lies at lower energy; in an electron transfer mechanism, the ordering of curves would be reversed. While the choice between ETM or covalent paths will be a function of structure and reaction medium, the two mechanisms will often follow very similar paths. In ETM, projecting along the electron transfer coordinate to the radical ion stage should thus be a reliable, if exaggerated, augur of many reaction features.

Some examples of ETM are trivial and require no computation. Dissociative electron transfer is well-known for some structure types.<sup>17a,24</sup> For example, the ETM description of nucleophilic aliphatic or aromatic substitution would transfer an electron from nucleophile to substrate (eq 2), giving a radical and radical anion; radical anions of (e.g.) alkyl or aryl halides are commonly dissociative. Although our focus here is on ground state reactions, electron transfer is well documented in photochemistry.<sup>17m,25</sup>

**Computational Methodology.** Our computational approach is operationally simple. For a polar bimolecular reaction, we choose the expected direction of electron transfer and optimize structures for relevant radicals or radical ions using DFT methods. In rare cases where directionality is ambiguous, we calculate the energetic consequences in both directions and choose the lower energy path. Sites of higher reactivity are

revealed by a composite spin density map (SDM) of odd electron character on the three-dimensional electron density surface, assuming that a new two-electron bond would occur preferentially at these sites. In the default color scheme, blue = highest spin and red = lowest spin. Each structure has a unique scale; we have not yet explored whether absolute spin densities are useful predictors of reactivity. Radicals, radical cations, and radical anions all utilize the same color scheme in the SDM. Importantly, no orbital pairs need be chosen because ETM treats the entire molecular structure; the sole initial question is *direction* of electron transfer. We note that the spin isosurface and SDM are not the same. Figure 3 shows these two surfaces

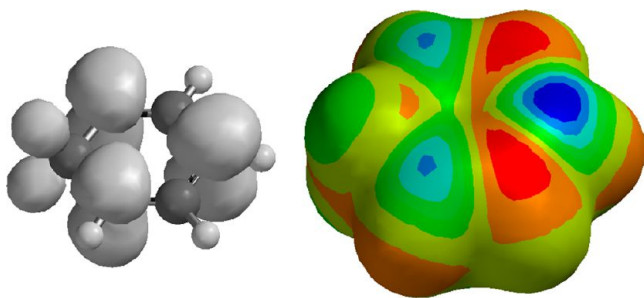


Figure 3. Spin isosurface and spin density map (SDM).

for the cyclohexadienyl radical, part of our treatment of the Birch reduction mechanism. The spin isosurface (at left) shows no obvious preference for a reactive site. By contrast, the SDM more subtly reveals the site of highest odd electron density (blue) on the outer fringe of the electron cloud; this is where protonation occurs in the related anion.

Optimizations were carried out with Spartan 10<sup>26</sup> or Gaussian 03 or 09,<sup>27</sup> using the Truhlar M05-2X functional and 6-31+G(d) basis set,<sup>28</sup> followed by vibrational frequency analysis. Other DFT methods gave similar results, but we have not yet carried out a systematic study. Visualizations are from Spartan 10 with the M05-2X functional and 6-31+G(d) basis set. In the default Spartan color scheme, reactive sites (high spin density) appear as bright blue. Conformational analysis can also be applied where necessary; this is critical for conformationally flexible reactants.

Variations on this method were explored. Lower level theories such as semiempirical or UHF/3-21G gave inconsistent results, presumably because of wave function spin-

contamination. Alternative visualizations might utilize either the SOMO or a direct map of the spin surface. In most cases, we find that the composite spin density map (SDM) described above provided the clearest result. Although neutral reactant geometries might be used, we quickly found that consideration of the geometric changes in radical ions is essential; this should point along the reaction coordinate in which electron density is accepted or donated by reactants. Indeed, this emerged as a general principle.

In the sections below, we show how ETM may be applied to representative examples of the reaction types in eqs 1–3. Our intention here is not to be encyclopedic but to demonstrate the power of this very simple method.

**Cycloadditions.** As shown by Houk and others, Diels–Alder regioselectivity is one legendary success of FMO theory.<sup>1a,3,6i,k,29</sup> For a “normal” electron demand Diels–Alder reaction, which matches an electron-poor dienophile and electron-rich diene, ETM would pair up the dienophile radical anion with the diene radical cation. “Inverse” electron demand Diels–Alder reactions make the opposite pairing. Dipolar [2 + 4] cycloadditions are also well treated by FMO methods.<sup>1a,3</sup>

**Diels–Alder Cycloadditions.** Typical regioselectivity for normal electron demand Diels–Alder reactions is illustrated in Figure 4. Below each reaction type are shown radical ion pairs for reactants, with structures optimized and then visualized as a SDM. Dienes substituted at C1 with an electron donating group (SDMs 1–3) usually give “ortho” products with dienophiles (7 and 8), whereas substitution at C2 (SDMs 4–6) gives “para” cycloadducts. In every case, matching the higher spin (blue) regions on the SDMs clearly reproduces observed regioselectivity.

Lewis acid complexation of the dienophile may not change this picture. As one example, Figure 5 shows the SDM of the BF<sub>3</sub>-acrolein complex radical anion in its lowest energy conformer. Spin density remains more heavily localized on C3.

Figure 6 presents the application of ETM to several [2 + 4] cycloadditions from the recent literature. In the first example, reported by Spanevello and co-workers, cyclopentadiene adds to a carbohydrate-derived nitro alkene to yield a mixture of *exo* and *endo* products.<sup>30</sup> Opposite faces of the dienophile radical anion SDM, **9a** and **9b**, are shown. Image **9a** predicts facial selectivity *syn* to both carbon–oxygen bonds, as observed by experiment. In the second example, as part of a synthesis of Peribysin-E, Danishefsky and co-workers reacted S-carvone with 2-trimethylsilyloxybutadiene, using Lewis acid catalysis.<sup>31</sup>

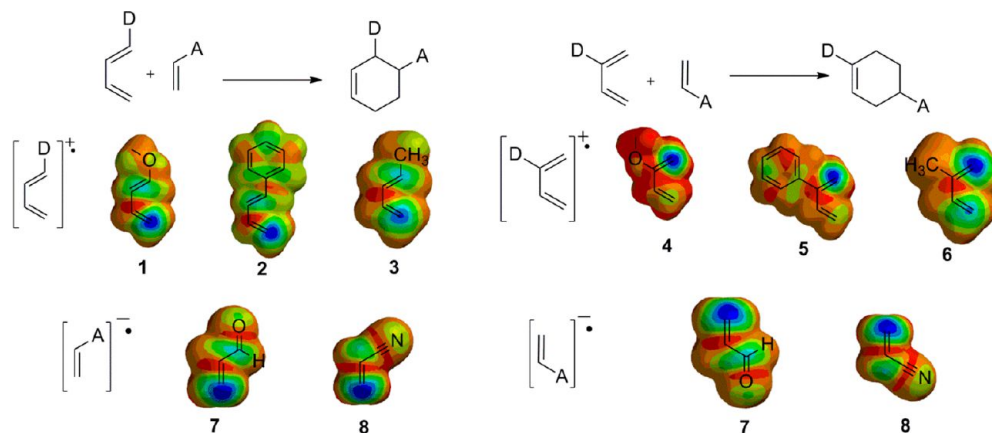


Figure 4. General modes of Diels–Alder regioselectivity.



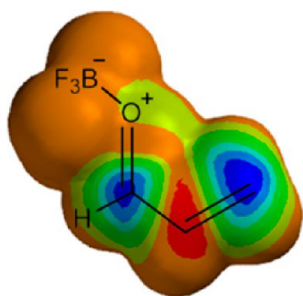


Figure 5. Radical anion of the  $\text{BF}_3$ -acrolein complex.

The observed regio- and stereoselectivity are rationalized by matching SDM 10a of the dienophile-catalyst radical anion with 11 from the diene radical cation.

#### Inverse Electron Demand Diels–Alder Cycloadditions.

As expected, ETM works equally well for inverse electron demand reactions. Examples are summarized in Figure 7. Dihydropyrans are commonly prepared by [2 + 4] cycloaddition of  $\alpha,\beta$ -unsaturated carbonyl derivatives with alkoxy alkenes.<sup>32</sup> Alignment of SDMs for the *S-cis* acrolein radical anion (12) and methoxyethylene radical cation (13) demonstrates the success of ETM in treating this type of reaction. One classic example is regioselective reaction of tropone with styrene to give a bicyclic product.<sup>33</sup> In this case, SDM surfaces for the tropone radical anion (14) and styrene radical cation (15) correctly match the observed regiochemistry. The third example is from our own recent report on thermal cycloaddition of indene with an *o*-quinol.<sup>34</sup> SDM visualizations for indene radical cation (16) and the quinol radical anion (17a vs 17b) reproduce the reaction regiochemistry and facial selectivity *syn* to the hydroxy substituent.

**Dipolar Cycloadditions.** Dipolar cycloadditions combine diverse groups of reactants.<sup>35</sup> While these reactions are likely to have a high degree of polarization, the directionality of electron transfer varies with structure type.<sup>35a</sup> For dipolar reactants, geometric changes in radical anions are found to be quite substantial. Figure 8 shows some of the examples we have explored to date. The first example shows a diazoester-enamine cycloaddition, in which the direction of electron transfer is unambiguous. Regiochemistry is clearly rationalized by matching SDMs for the enamine radical cation (18) with diazoester radical anion (19).<sup>36</sup> We note substantial in-plane bending of 19 in the direction of reaction. The second example represents a common type of azide–alkyne cycloaddition

chemistry.<sup>37</sup> Both directions of electron transfer were investigated, and the lower energy solution by 10.8 kcal/mol is shown. Matching SDMs for the azide radical cation (20) and dipolarophile radical anion (21) reproduces regiochemistry of the major product.<sup>38</sup> In the third example, DeShong and co-workers used a chiral nitron in a regio- and stereoselective cycloaddition with ethyl vinyl ether as the key step in the synthesis of the amino sugar daunosamine.<sup>39</sup> This case required conformational analysis of the nitron radical anion, which is substantially pyramidalized at the nitron carbon. Matching SDMs 22 (shown sideways) and 23 reproduces observed regiochemistry and facial selectivity for addition to the dipole.

**Ketene [2 + 2] Cycloadditions.** Ketene cycloadditions are highly polar, with the ketene component typically playing the role of electron-acceptor.<sup>40</sup> One important observation is that ketene radical anions undergo substantial in-plane bending (Figure 9) because the ketene LUMO lies in the molecular plane. In the first example, reported by Brady,<sup>41</sup> paired SDMs for an alkene radical cation (24) and dichloroketene radical anion (25) correctly assign the major product. In the second example Correia and co-workers reacted an alkyl-substituted ketene with an enecarbamate as a key step toward indolizidine-type structures; spin density surfaces 26 and 27 reproduce the regiochemistry of this reaction.<sup>42</sup> In this case, there are two modes of ketene bending; the lower energy solution is shown.

**Electrophilic Additions.** In the ETM description of electrophilic additions (eq 3), we first transfer an electron from substrate to electrophile. Computational models for the substrate radical cation should thus be most informative. Figure 10 illustrates how the preferred site of electrophilic addition is easily predicted by radical cation SDMs for conjugated and unconjugated alkenes, alkynes, and polyenes (28–34). As expected, SDMs for the radical cations of carbonyl species (35 and 36) predict that electrophilic interaction will occur at the carbonyl oxygen in the plane of the C–O  $\pi$  bond. More subtle facial selectivity of electrophilic addition is observed in bicyclic alkenes. In the first example shown, the exocyclic  $\pi$  bond twists slightly and bends toward the ring  $\pi$  bond; this leads to greater spin density on the *exo* face (SDM 37a vs 37b), consistent with observed stereochemistry.<sup>43</sup> For the well-studied case of norbornene, which is slightly pyramidalized in the neutral structure,<sup>44</sup> the radical cation is flatter (SDMs 38a and 38b) and computational reproduction of an *exo* preference is due to hyperconjugation of the SOMO with C1–C6 and C4–C5  $\sigma$  bonds.

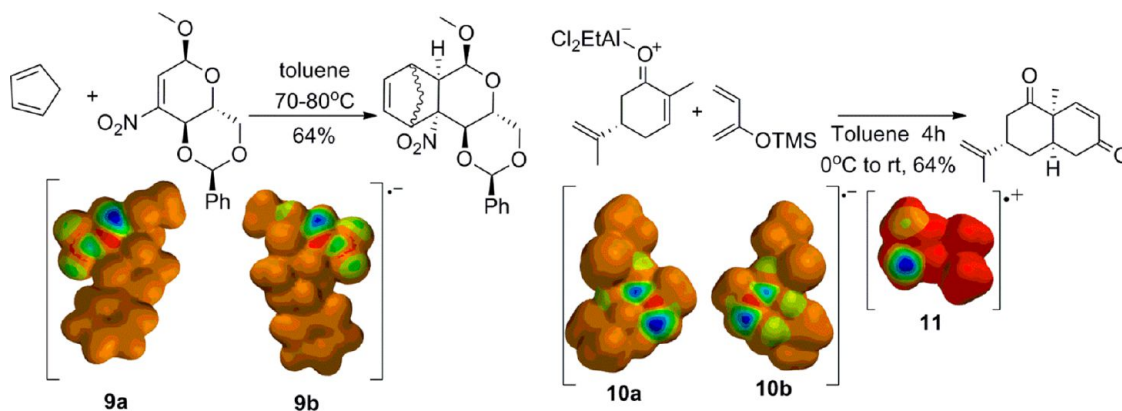


Figure 6. Recent examples of Diels–Alder regioselectivity.

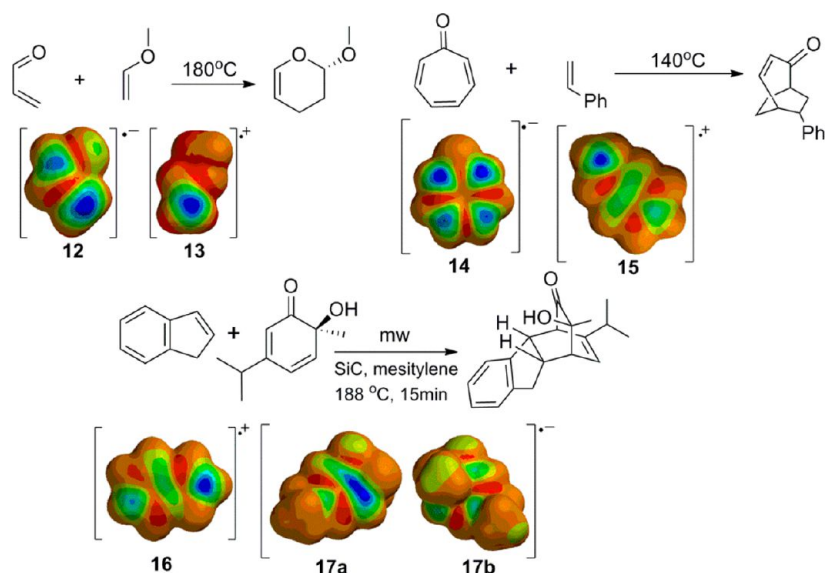


Figure 7. ETM results for inverse electron demand Diels–Alder reactions.

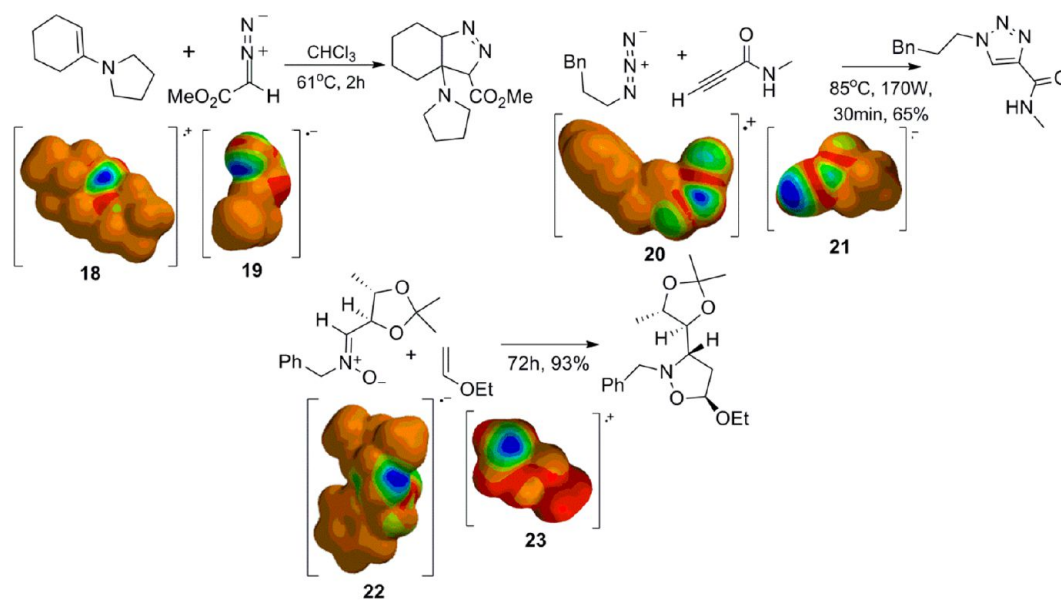


Figure 8. ETM results for dipolar cycloadditions.

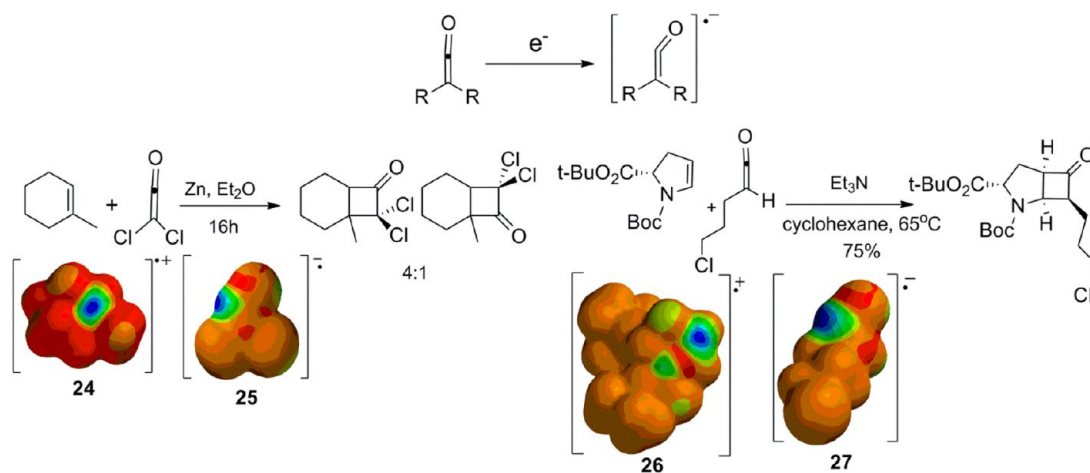


Figure 9. ETM results for ketene cycloadditions.

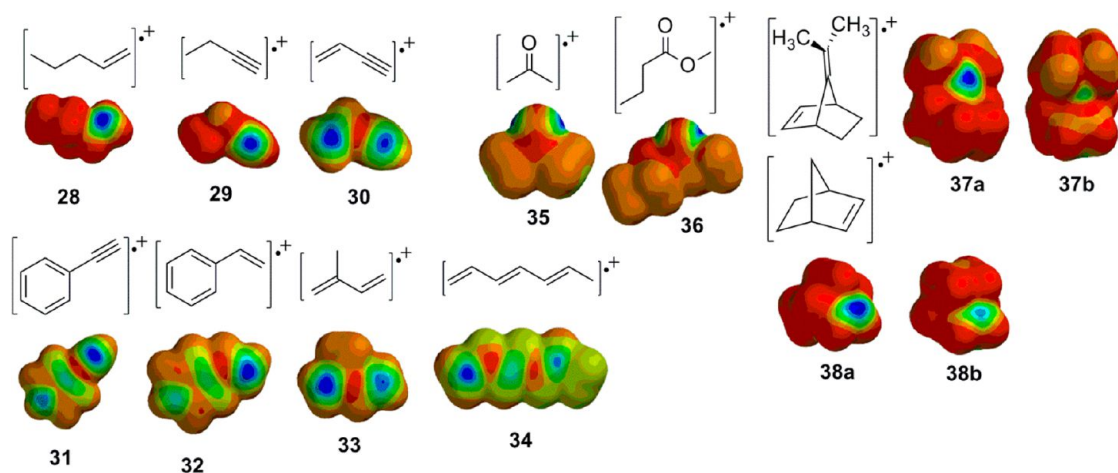


Figure 10. ETM results for electrophilic additions to alkenes, alkynes, polyenes, and carbonyl compounds.

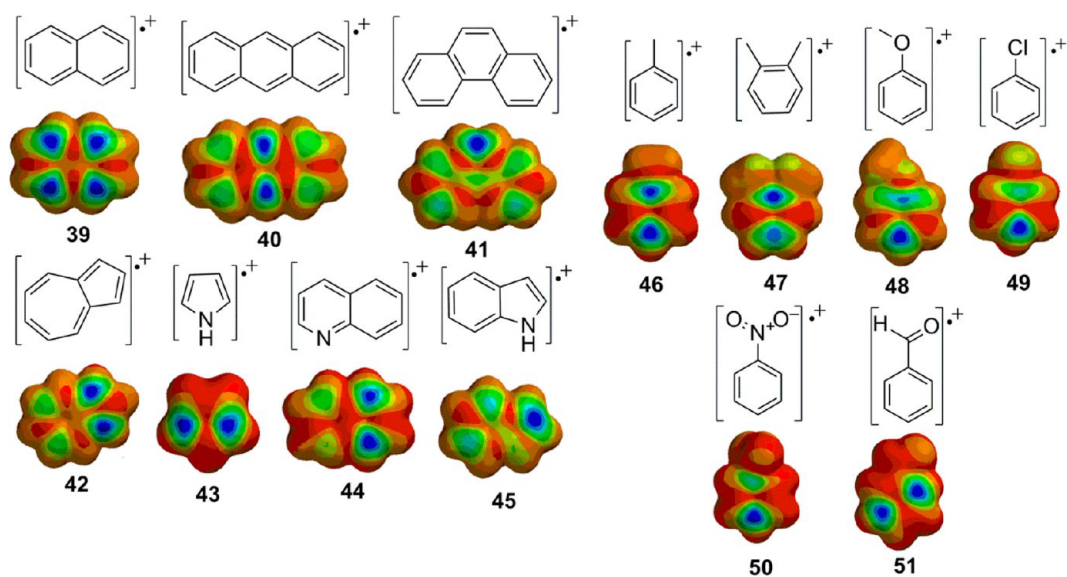


Figure 11. ETM results for electrophilic aromatic substitution.

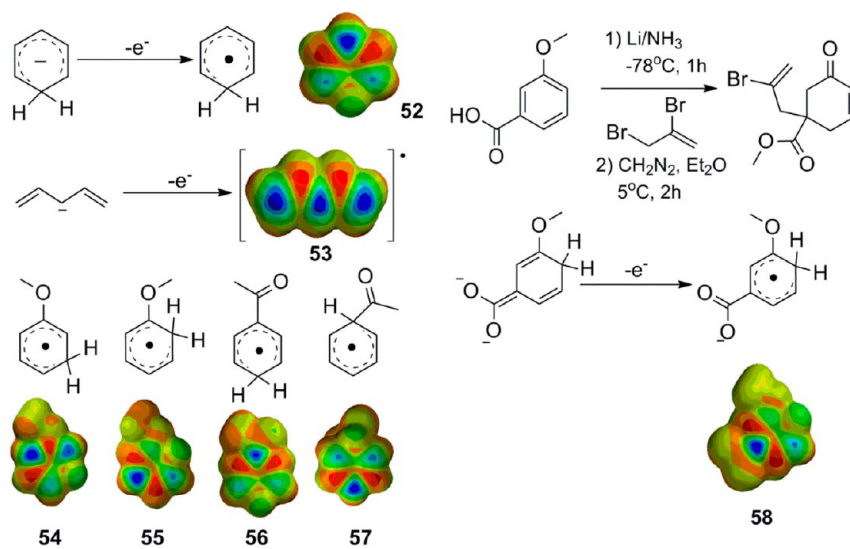


Figure 12. ETM description of the Birch reduction.



The possibility of an electron transfer mechanism for some electrophilic aromatic substitutions (EAS) has been discussed previously by Kochi.<sup>17c,45</sup> ETM predictions for polycyclic aromatics (SDMs 39–45, Figure 11) are unambiguous and consistent with experiment. Substituted aromatics provide some unanticipated results. With toluene (46), *o*-xylene (47), or anisole (48), *para* and *ipso* addition are predicted by spin densities in the radical cations. This may seem inconsistent with experiment; in fact, the *ipso* addition of electrophiles is well documented.<sup>46</sup> Our results support the secondary rearrangement of initial *ipso* sigma complexes as a source of *ortho* products. Chlorobenzene (SDM 49) follows this trend. Not surprisingly, electron-poor aromatics fail to give predictions consistent with experiment. The radical cation of nitrobenzene (50) shows greatest spin density at sites *ortho* and *para* to the substituent while benzaldehyde radical cation (51) incorrectly predicts *ortho* + *meta* products.

Regioselectivity in the Birch reduction<sup>47</sup> presents a difficult challenge to theory, as discussed in a recent review by Zimmerman.<sup>48</sup> The first protonation step cannot be addressed by ETM since this requires modeling a neutral reactant that has no odd spin density. Product regiochemistry derives from the second step, protonation of a pentadienyl anion. Zimmerman correlated the site of protonation with anion electron densities.<sup>48,49</sup> In ETM, this would be modeled by SDMs for the neutral radicals, which are shown here. The SDM for cyclohexadienyl radical (52, Figure 12) reproduces observed protonation at the central carbon to afford 1,4-cyclohexadiene. It is interesting that ETM predicts little selectivity in electrophilic additions to acyclic pentadienyl anion (SDM 53); this also is consistent with experiment.<sup>50</sup> With methoxy or acyl substitution (SDMs 54–57), ETM reproduces the product regiochemistry, regardless of the site of initial radical anion protonation. The final example is from a recent synthesis by Williams and co-workers in which the key step is electrophilic alkylation of a dianion. In this case, spin density on the associated radical anion 58 (dianion minus one electron) reproduces the observed site of alkylation.<sup>51</sup>

**Nucleophilic Additions.** In the ETM description for nucleophilic addition (eq 2), an electron is first transferred from nucleophile to substrate, followed by bonding between the radical and radical anion. Since there is little mystery about odd electron character in most radicals, we focus here on finding the optimal geometry for the substrate radical anion and visualizing the SDM. This may have a single solution or require more complex conformational analysis for many reactions of synthetic interest.

SDMs for radical anions of some common nucleophilic substrates (59–64) are assembled in Figure 13. Radical anions of simple nitriles,<sup>52</sup> alkynes,<sup>53</sup> carbonyl derivatives,<sup>54</sup> and imines<sup>54a</sup> all have been predicted earlier to undergo substantial bending or pyramidalization; these geometric changes portend the product geometry and thus reveal the site of nucleophilic addition.

Garg and Houk have investigated nucleophilic additions to indolynes and related benzyne analogs.<sup>55</sup> Regioselectivity is predicted from the optimized aryne geometry. The more linear and strained aryne terminus is found to be more reactive. Figure 14 shows the application of ETM to several indolynes. The observed percent reactivity of each site for nucleophilic addition of aniline correlates well with spin density in the radical anions 65–67. As with the neutral structures, the more reactive sites in radical anions have larger bond angles.

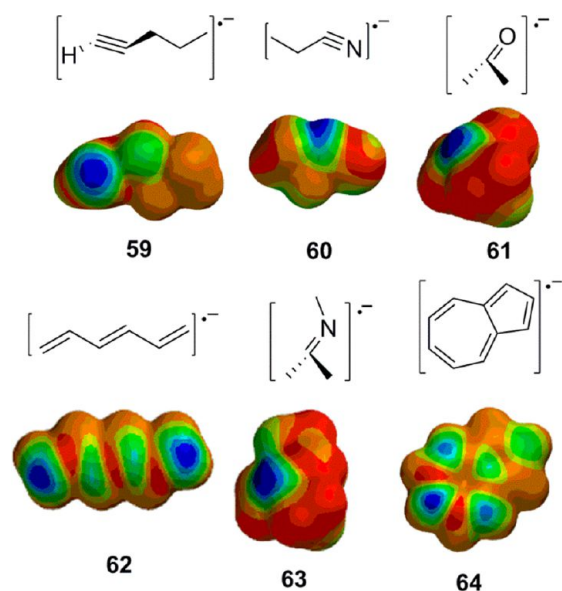


Figure 13. ETM results for simple nucleophilic additions.

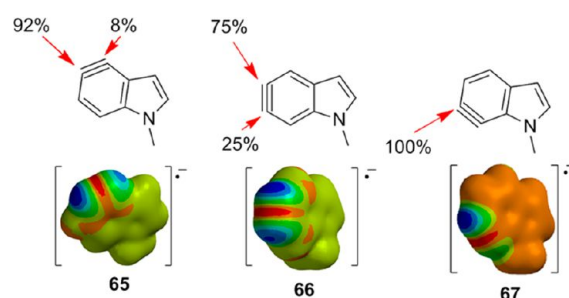
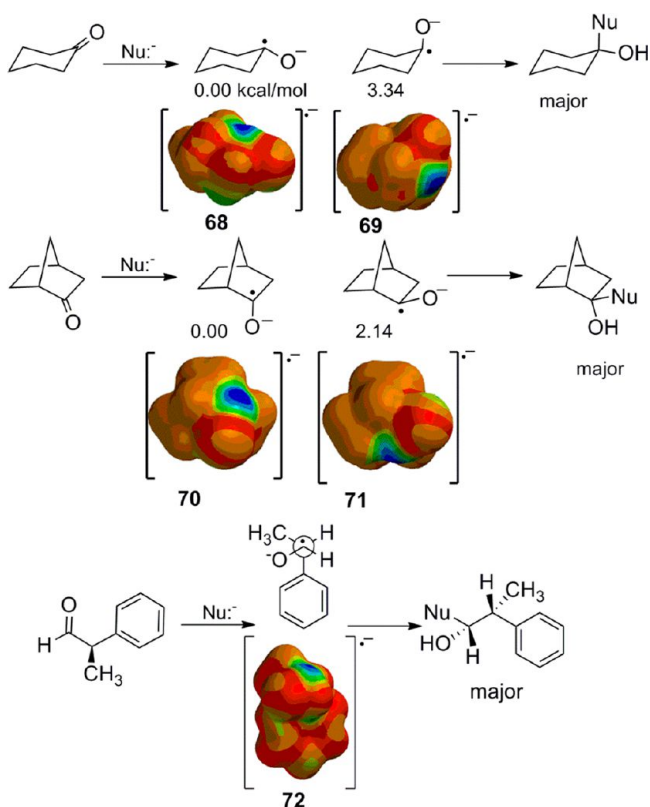


Figure 14. Nucleophilic addition to indolynes.

Numerous arguments have been made for the origins of stereoselectivity in nucleophilic additions to cyclic ketones.<sup>1a,10c,11,13b,c,56</sup> Applying our ETM approach, we find that multiple minima usually exist for carbonyl radical anions; the lowest energy structure predicts addition stereochemistry. Two examples are shown in Figure 15. For cyclohexanone radical anion, two chair conformers exist, as well as a twist-boat conformer at higher energy. The SDM for the lowest energy conformer (68) reproduces the known preference for axial addition. With norbornanone, the lower energy conformer (SDM 70) reproduces *exo* nucleophilic attack since pyramidalization bends the oxygen toward the *endo* face. Conformational analysis also succeeds for acyclic substrates. 2-Phenylpropanal is commonly cited as an example for diastereoselective addition. A full search of the radical anion conformational space reveals the lowest energy conformer to be represented as 72. This leads to the observed stereochemistry and is most consistent with the Felkin–Ahn analysis of transition state structures.<sup>13b,57</sup>

Nucleophilic addition or one-electron reduction both add electron density, and the structure responds in each case by distorting in the same direction. The origin of these conformational preferences must lie in hyperconjugation<sup>58</sup> with proximate C–C or C–H bonds. The dominant interaction appears to be delocalization of the singly occupied MO (SOMO), which favors hyperconjugation with C–H bonds. Acyclic example 72 is more complex since the SOMO shows



**Figure 15.** ETM results for diastereoselective nucleophilic additions to ketones.

delocalization into the phenyl group. More detailed analysis of these effects will be reported at a later time.

The radical anion of acrolein is flat (SDM 7). Radical anions of cyclohexenones exist in a half-chair conformation similar to the neutral structure and show negligible pyramidalization at C3. The  $\pi$  face that is *syn* to the out-of-plane C5 methylene is predicted to be more receptive to nucleophiles. With a methyl group at C5 in a pseudoequatorial conformation, *trans*-addition is predicted by SDM 73a (Figure 16), consistent with results reported by Allinger.<sup>59</sup> The second example of a more complex tricyclic enone shows slightly greater pyramidalization, with SDM 74a in agreement with known addition to the *exo* face.<sup>60</sup>

**A Structure-Reaction Coordinate Principle for Electron Transfer.** According to the structure-correlation principle, nascent structural changes along a chemical reaction coordinate are revealed in the reactant geometry as subtle deviations of bond distances and angles from normal values.<sup>12</sup> This is most commonly studied by X-ray crystal structures or computation. ETM is less subtle because it overshoots the likely transition state but provides information about geometric changes along a reaction coordinate.

A similar general principle emerges from our ETM analysis: One-electron oxidation or reduction often engenders electronic and geometric changes that parallel the reaction coordinate for electrophilic or nucleophilic addition, respectively. The effect is more dramatic for one-electron reduction. For example, carbonyl radical anions pyramidalize, with ligands moving in the direction opposite to nucleophilic addition. This observation may help to explain the origins of the well-known Bürgi–Dunitz trajectory for nucleophilic addition to carbonyl groups.<sup>61</sup> Ketene, alkyne, and nitrile radical anions bend, again in a direction indicative of cycloaddition or nucleophilic

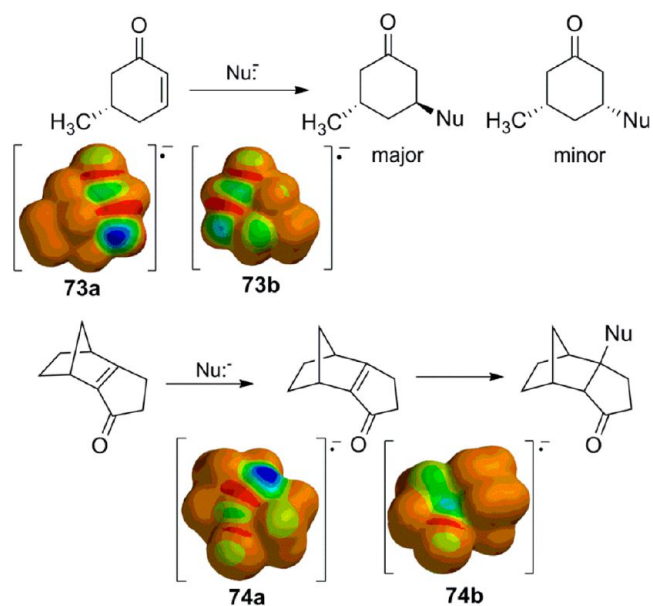


**Figure 16.** ETM results for nucleophilic additions to conjugated systems.

addition. Geometric changes in radical cations are more subtle but can still be informative.

## CONCLUSIONS

It has long been recognized that many bimolecular reactions begin as charge-transfer complexes and proceed with a high degree of electron transfer. FMO theory is predicated on this concept but underestimates the degree of electron transfer and provides no information about impending changes in reactant geometries.<sup>6</sup> As noted 25 years ago by Pross,<sup>22</sup> single-electron shift processes provide an excellent description of nucleophilic and electrophilic additions. We have explored the consequences of *systematically* transferring one electron, using DFT computations to optimize structures of the radical or radical ion intermediates and matching spin density maps (SDMs) to predict reactive sites. We find that this electron transfer model (ETM) reproduces observed regio- and stereochemistry for a broad array of reactions, including Diels–Alder, dipolar and ketene cycloadditions, Birch reduction, many types of nucleophilic additions, and electrophilic addition to aromatic rings and polyenes. This conceptually simple but powerful method almost certainly works because the electronic and geometric changes due to one electron oxidation or reduction clarify the effects of polarization and may parallel the reaction coordinate for electrophilic or nucleophilic addition, respectively. The broad success of ETM suggests that many polar reactions may follow a mechanism closer to inner-shell single electron transfer than is generally believed.

We have applied a systematic electron transfer model (ETM) to many common organic reactions but the general principles described here should be equally applicable to inorganic or biological structures. We are continuing to explore the applications and limitations of this method.

## ASSOCIATED CONTENT

### Supporting Information

Cartesian coordinates and energies for radical and radical ion stationary points. This material is available free of charge via the Internet at <http://pubs.acs.org>.



## ■ AUTHOR INFORMATION

## Corresponding Author

\*E-mail: Richard.Johnson@unh.edu.

## Notes

The authors declare no competing financial interest.

## ■ ACKNOWLEDGMENTS

We are grateful for generous support from the National Science Foundation (CHE-0910826) and to a reviewer for suggesting the application of ETM to indolynes chemistry.

## ■ DEDICATION

This paper is dedicated to the memory of Professor Howard E. Zimmerman.

## ■ REFERENCES

- (1) (a) Fleming, I. *Molecular Orbitals and Organic Chemical Reactions*, Reference ed.; John Wiley & Sons: New York, 2010. (b) Fleming, I., *Frontier Orbitals and Organic Chemical Reactions*; John Wiley & Sons: New York, 1976; 249 pp.
- (2) Houk, K. N.; Paddon-Row, M. N.; Rondan, N. G.; Wu, Y. D.; Brown, F. K.; Spellmeyer, D. C.; Metz, J. T.; Li, Y.; Loncharich, R. J. *Science* **1986**, *231*, 1108–1117.
- (3) Ess, D. H.; Jones, G. O.; Houk, K. N. *Adv. Synth. Catal.* **2006**, *348*, 2337–2361.
- (4) (a) Corbeil, C. R.; Moitessier, N. *J. Mol. Catal. A Chem.* **2010**, *324*, 146–155. (b) Weill, N.; Corbeil, C. R.; De Schutter, J. W.; Moitessier, N. *J. Comput. Chem.* **2011**, *32*, 2878–2889. (c) Brown, J. M.; Deeth, R. *J. Angew. Chem., Int. Ed.* **2009**, *48*, 4476–4479. (d) Houk, K. N.; Cheong, P. H.-Y. *Nature (London, U.K.)* **2008**, *455*, 309–313.
- (5) (a) van Zeist, W.-J.; Bickelhaupt, F. M. *Org. Biomol. Chem.* **2010**, *8*, 3118–3127. (b) Hayden, A. E.; Houk, K. N. *J. Am. Chem. Soc.* **2009**, *131*, 4084–4089.
- (6) (a) Fukui, K. *Angew. Chem.* **1982**, *94*, 852–861. (b) Fukui, K. *Science* **1982**, *218*, 747–754. (c) Fukui, K. *Pure Appl. Chem.* **1982**, *54*, 1825–1836. (d) Fujimoto, H.; Fukui, K. *Chemical Reactivity and Reaction Paths*; Wiley-Interscience: New York, 1974; pp 23–54. (e) Fukui, K. *Acc. Chem. Res.* **1971**, *4*, 57–64. (f) Fukui, K.; Fujimoto, H. *Bull. Chem. Soc. Jpn.* **1969**, *42*, 3399–3409. (g) Fukui, K.; Fujimoto, H. *Bull. Chem. Soc. Jpn.* **1967**, *40*, 2018–2025. (h) Rozeboom, M. D.; Tegmo-Larsson, I. M.; Houk, K. N. *J. Org. Chem.* **1981**, *46*, 2338–45. (i) Houk, K. N. *Acc. Chem. Res.* **1975**, *8*, 361–369. (j) Chao, T. M.; Baker, J.; Hehre, W. J.; Kahn, S. D. *Pure Appl. Chem.* **1991**, *63*, 283–288. (k) Kahn, S. D.; Pau, C. F.; Overman, L. E.; Hehre, W. J. *J. Am. Chem. Soc.* **1986**, *108*, 7381–96. (l) Salem, L. *J. Am. Chem. Soc.* **1968**, *90*, 543–552. (m) Klopman, G. *J. Am. Chem. Soc.* **1968**, *90*, 223–234.
- (7) (a) Parr, R. G.; Chattaraj, P. K. *J. Am. Chem. Soc.* **1991**, *113*, 1854–1855. (b) Parr, R. G.; Pearson, R. G. *J. Am. Chem. Soc.* **1983**, *105*, 7512–7516. (c) Pearson, R. G.; Songstad, J. *J. Am. Chem. Soc.* **1967**, *89*, 1827–1836. (d) Pearson, R. G. *J. Am. Chem. Soc.* **1963**, *85*, 3533–3539. (e) Geerlings, P.; De Proft, F. *Int. J. Quantum Chem.* **2000**, *80*, 227–235.
- (8) (a) Geerlings, P.; De Proft, F. *Phys. Chem. Chem. Phys.* **2008**, *10*, 3028–3042. (b) Geerlings, P.; De Proft, F.; Langenaeker, W. *Chem. Rev.* **2003**, *103*, 1793–1873. (c) Domingo, L. R.; Aurell, M. J.; Perez, P.; Contreras, R. *J. Phys. Chem. A* **2002**, *106*, 6871–6875. (d) Geerlings, P.; Ayers, P. W.; Toro-Labbé, A.; Chattaraj, P. K.; De Proft, F. *Acc. Chem. Res.* **2012**, *45*, 683–695.
- (9) (a) Cardenas, C.; Rabi, N.; Ayers, P. W.; Morell, C.; Jaramillo, P.; Fuentealba, P. *J. Phys. Chem. A* **2009**, *113*, 8660–8667. (b) Chattaraj, P. K.; Sarkar, U.; Roy, D. R. *Chem. Rev.* **2006**, *106*, 2065–2091. (c) Li, Y.; Evans, J. N. S. *J. Am. Chem. Soc.* **1995**, *117*, 7756–7759.
- (10) (a) Ohwada, T. *Top. Curr. Chem.* **2009**, *289*, 129–181. (b) Inagaki, S. *Top. Curr. Chem.* **2009**, *289*, 57–82. (c) Ohwada, T. *Chem. Rev.* **1999**, *99*, 1337–1375. (d) Burgess, E. M.; Liotta, C. L. *J. Org. Chem.* **1981**, *46*, 1703–1708.
- (11) Tomoda, S. *Chem. Rev.* **1999**, *99*, 1243–1263.
- (12) (a) Bürgi, H. B. *Acta Crystallogr., Sect. A: Found. Crystallogr.* **1998**, *A54*, 873–885. (b) Bürgi, H.-B.; Shklover, V. *Organometallic and Organometalloidal Compounds*. In *Structure Correlation*; VCH: Weinheim, 1994; Vol. 1, pp 303–335. (c) Bürgi, H. B.; Dunitz, J. D. *Acc. Chem. Res.* **1983**, *16*, 153–161.
- (13) (a) Mehta, G.; Uma, R. *Acc. Chem. Res.* **2000**, *33*, 278–286. (b) Mehta, G.; Chandrasekhar, J. *Chem. Rev.* **1999**, *99*, 1437–1467. (c) Dannenberg, J. J. *Chem. Rev.* **1999**, *99*, 1225–1241. (d) Ganguly, B.; Chandrasekhar, J.; Khan, F. A.; Mehta, G. *J. Org. Chem.* **1993**, *58*, 1734–1739.
- (14) (a) Mulliken, R. S. *J. Am. Chem. Soc.* **1952**, *74*, 811–284. (b) Morokuma, K. *Acc. Chem. Res.* **1977**, *10*, 294–300. (c) Rosokha, S. V.; Kochi, J. K. *J. Org. Chem.* **2002**, *67*, 1727–1737.
- (15) Rosokha, S. V.; Kochi, J. K. *Acc. Chem. Res.* **2008**, *41*, 641–653.
- (16) (a) Fuentealba, P.; Florez, E.; Tiznado, W. *J. Chem. Theory Comput.* **2010**, *6*, 1470–1478. (b) Langenaeker, W.; Demel, K.; Geerlings, P. *J. Mol. Struct. THEOCHEM* **1991**, *80*, 329–342. (c) Yang, W.; Parr, R. G.; Pucci, R. *J. Chem. Phys.* **1984**, *81*, 2862–2863. (d) Komorowski, L.; Lipinski, J.; Szarek, P.; Ordon, P. *J. Chem. Phys.* **2011**, *135*, 014109/1–014109/8. (e) Bultinck, P.; Clarisse, D.; Ayers, P. W.; Carbo-Dorca, R. *Phys. Chem. Chem. Phys.* **2011**, *13*, 6110–6115.
- (17) (a) Houmam, A. *Chem. Rev.* **2008**, *108*, 2180–2237. (b) Antonello, S.; Maran, F. *Chem. Soc. Rev.* **2005**, *34*, 418–428. (c) Gwaltney, S. R.; Rosokha, S. V.; Head-Gordon, M.; Kochi, J. K. *J. Am. Chem. Soc.* **2003**, *125*, 3273–3283. (d) Fukuzumi, S. In *Electron Transfer in Chemistry*; Wiley-VCH: Weinheim, 2001; Vol. 4, pp 3–67. (e) Nelsen, S. F. In *Electron Transfer in Chemistry*; Balzani, V., Piotrowski, P., Eds.; Wiley-VCH: Weinheim, 2001; Vol. 1, pp 342–392. (f) Speiser, B. *Angew. Chem., Int. Ed. Engl.* **1996**, *35*, 2471–2474. (g) Sastry, G. N.; Reddy, A. C.; Shaik, S. *Angew. Chem., Int. Ed. Engl.* **1995**, *34*, 1495–1497. (h) Lund, H.; Daasbjerg, K.; Lund, T.; Pedersen, S. U. *Acc. Chem. Res.* **1995**, *28*, 313–19. (i) Saveant, J. M. *Acc. Chem. Res.* **1993**, *26*, 455–461. (j) Ebersson, L.; Shaik, S. S. *J. Am. Chem. Soc.* **1990**, *112*, 4484–4489. (k) Ashby, E. C. *Acc. Chem. Res.* **1988**, *21*, 414–421. (l) Ebersson, L. *Electron Transfer Reactions in Organic Chemistry*; Springer-Verlag: New York, 1988. (m) Mariano, P. S., Ed.; *Advances in Electron Transfer Chemistry*; JAI Press: New York, 1999; Vol. 6.
- (18) Marcus, R. A.; Sutin, N. *Biochim. Biophys. Acta* **1985**, *811*, 265–322.
- (19) Dewar, M. J. S. *J. Mol. Struct. THEOCHEM* **1989**, *59*, 301–323.
- (20) (a) Donoghue, P. J.; Wiest, O. *Chem.—Eur. J.* **2006**, *12*, 7018–7026. (b) Ischay, M. A.; Yoon, T. P. *Eur. J. Org. Chem.* **2012**, *2012*, 3359–3372. (c) Baumgarten, M.; Muellen, K. *Top. Curr. Chem.* **1994**, *169*, 1–103.
- (21) (a) Hammes-Schiffer, S.; Stuchebrukhov, A. A. *Chem. Rev.* **2010**, *110*, 6939–6960. (b) Huynh, M. H. V.; Meyer, T. J. *Chem. Rev.* **2007**, *107*, 5004–5064.
- (22) (a) Pross, A.; Chipman, D. M. *Free Radical Biol. Med.* **1987**, *3*, 55–64. (b) Pross, A. *Adv. Chem. Ser.* **1987**, *215*, 331–338. (c) Pross, A. *Acc. Chem. Res.* **1985**, *18*, 212–219.
- (23) Pross, A.; Shaik, S. S. *Acc. Chem. Res.* **1983**, *16*, 363–370.
- (24) Saveant, J. M. *J. Electroanal. Chem.* **2000**, *485*, 86–88.
- (25) (a) Cho, D. W.; Yoon, U. C.; Mariano, P. S. *Acc. Chem. Res.* **2011**, *44*, 204–215. (b) Griesbeck, A. G.; Hoffmann, N.; Warzecha, K.-d. *Acc. Chem. Res.* **2007**, *40*, 128–140. (c) Hoffmann, N. *J. Photochem. Photobiol., C* **2008**, *9*, 43–60.
- (26) *Spartan 10*; Wavefunction Inc.: Irvine, CA, 2011; Version 1.1.
- (27) (a) Frisch, M. J. et al. *Gaussian 03*, Revision E.01; Gaussian Inc.: Wallingford, CT, 2004. (b) Frisch, M. J. et al. *Gaussian 09*, Revision B.01; Gaussian Inc.: Wallingford, CT, 2010.
- (28) Zhao, Y.; Truhlar, D. G. *Acc. Chem. Res.* **2008**, *41*, 157–167.
- (29) Houk, K. N.; Gonzalez, J.; Li, Y. *Acc. Chem. Res.* **1995**, *28*, 81–90.
- (30) Mangione, M. I.; Sarotti, A. M.; Suárez, A. G.; Spanevello, R. A. *Carbohydr. Res.* **2011**, *346*, 460–464.

- (31) Angeles, A. R.; Waters, S. P.; Danishefsky, S. J. *J. Am. Chem. Soc.* **2008**, *130*, 13765–13770.
- (32) Smith, C. W.; Norton, D. G.; Ballard, S. A. *J. Am. Chem. Soc.* **1951**, *73*, 5273–5280.
- (33) Uyehara, T.; Kitahara, Y. *Chem. Ind. (London)* **1971**, 354–355.
- (34) Dong, S.; Cahill, K. J.; Kang, M.-I.; Colburn, N. H.; Henrich, C. J.; Wilson, J. A.; Beutler, J. A.; Johnson, R. P.; Porco, J. A. *J. Org. Chem.* **2011**, *76*, 8944–8954.
- (35) (a) Engels, B.; Christl, M. *Angew. Chem., Int. Ed.* **2009**, *48*, 7968–7970. (b) Sustmann, R. *Heterocycles* **1995**, *40*, 1–18. (c) Huisgen, R. *Adv. Cycloaddit.* **1988**, *1*, 1–31. (d) Sustmann, R. *Tetrahedron Lett.* **1971**, 2717–2720. (e) Lan, Y.; Zou, L.; Cao, Y.; Houk, K. N. *J. Phys. Chem. A* **2011**, *115*, 13906–13920.
- (36) Piozzi, F.; Umami-Ronchi, A.; Merlini, L. *Gazetta* **1965**, 814–819.
- (37) (a) Kolb, H. C.; Sharpless, K. B. *Drug Discovery Today* **2003**, *8*, 1128–1137. (b) Kolb, H. C.; Finn, M. G.; Sharpless, K. B. *Angew. Chem., Int. Ed.* **2001**, *40*, 2004–2021.
- (38) Katritzky, A. R.; Singh, S. K. *J. Org. Chem.* **2002**, *67*, 9077–9079.
- (39) DeShong, P.; Dicken, C. M.; Leginus, J. M.; Whittle, R. R. *J. Am. Chem. Soc.* **1984**, *106*, 5598–5602.
- (40) Hyatt, J. A.; Reynolds, P. W. *Org. React. (N.Y.)* **1994**, *45*, 159–646.
- (41) Bak, D. A.; Brady, W. T. *J. Org. Chem.* **1979**, *44*, 107–110.
- (42) Valle, M. S.; Retailleau, P.; Correia, C. R. D. *Tetrahedron Lett.* **2008**, *49*, 1957–1960.
- (43) Mehta, G.; Gunasekaran, G.; Gadre, S. R.; Shirsat, R. N.; Ganguly, B.; Chandrasekhar, J. *J. Org. Chem.* **1994**, *59*, 1953–1955.
- (44) (a) Houk, K. N.; Rondan, N. G.; Brown, F. K. *Isr. J. Chem.* **1983**, *23*, 3–9. (b) Borden, W. T. *Chem. Rev.* **1989**, *89*, 1095–1109.
- (45) Rosokha, S. V.; Kochi, J. K. *J. Am. Chem. Soc.* **2001**, *123*, 8985–8999.
- (46) (a) Geppert, J. T.; Johnson, M. W.; Myhre, P. C.; Woods, S. P. *J. Am. Chem. Soc.* **1981**, *103*, 2057–2062. (b) Feldman, K. S.; Myhre, P. C. *J. Am. Chem. Soc.* **1979**, *101*, 4768–4769. (c) Barnes, C. E.; Myhre, P. C. *J. Am. Chem. Soc.* **1978**, *100*, 973–975. (d) Gibbs, H. W.; Moodie, R. B.; Schofield, K. J. *Chem. Soc., Chem. Commun.* **1976**, 492–493. (e) Hahn, R. C.; Strack, D. L. *J. Am. Chem. Soc.* **1974**, *96*, 4335–4337.
- (47) Rabideau, P. W.; Marcinow, Z. *Org. React. (N.Y.)* **1992**, *42*, 1–334.
- (48) Zimmerman, H. E. *Acc. Chem. Res.* **2012**, *45*, 164–170.
- (49) (a) Zimmerman, H. E.; Wang, P. A. *J. Am. Chem. Soc.* **1993**, *115*, 2205–2216. (b) Zimmerman, H. E.; Wang, P. A. *J. Am. Chem. Soc.* **1990**, *112*, 1280–1281. (c) Zimmerman, H. E. *Tetrahedron* **1961**, *16*, 169–176.
- (50) Nakamura, A.; Yasuda, H. *J. Organomet. Chem.* **1985**, *285*, 15–29.
- (51) Chow, S.; Kreß, C.; Albæk, N.; Jessen, C.; Williams, C. M. *Org. Lett.* **2011**, *13*, 5286–5289.
- (52) (a) Clark, T. *Faraday Discuss. Chem. Soc.* **1984**, *78*, 203–212. (b) Gutsev, G. L.; Sobolewski, A. L.; Adamowicz, L. *Chem. Phys.* **1995**, *196*, 1–11. (c) Timerghazin, Q. K.; Peslherbe, G. H. *J. Phys. Chem. B* **2008**, *112*, 520–528.
- (53) (a) Huang, M.-B.; Liu, Y. *J. Phys. Chem. A* **2001**, *105*, 923–929. (b) Damrauer, R. *J. Org. Chem.* **2006**, *71*, 9165–9171.
- (54) (a) Fourre, I.; Silvi, B.; Chaquin, P.; Sevin, A. *J. Comput. Chem.* **1999**, *20*, 897–910. (b) Koeppel, R.; Kasai, P. H. *J. Phys. Chem.* **1994**, *98*, 12904–12910. (c) Davies, A. G.; Neville, A. G. *J. Chem. Soc., Perkin Trans. 2* **1992**, 163–169.
- (55) (a) Goetz, A. E.; Bronner, S. M.; Cisneros, J. D.; Melamed, J. M.; Paton, R. S.; Houk, K. N.; Garg, N. K. *Angew. Chem., Int. Ed.* **2012**, *51*, 2758–2762. (b) Im, G. Y. J.; Bronner, S. M.; Goetz, A. E.; Paton, R. S.; Cheong, P. H. Y.; Houk, K. N.; Garg, N. K. *J. Am. Chem. Soc.* **2010**, *132*, 17933–17944.
- (56) (a) Li, H.; Le Noble, W. J. *Recl. Trav. Chim. Pays-Bas* **1992**, *111*, 199–210. (b) Cieplak, A. S. *J. Am. Chem. Soc.* **1981**, *103*, 4540–4552. (c) Klein, J. *Tetrahedron Lett.* **1973**, 4307–4310.
- (57) (a) Huet, J.; Maroni-Barnaud, Y.; Nguyen Trong, A.; Seyden-Penne, J. *Tetrahedron Lett.* **1976**, 159–162. (b) Cherest, M.; Felkin, H. *Tetrahedron Lett.* **1971**, 383–386. (c) Rosenberg, R. E.; Abel, R. L.; Drake, M. D.; Fox, D. J.; Ignatz, A. K.; Kwiat, D. M.; Schaal, K. M.; Virkler, P. R. *J. Org. Chem.* **2001**, *66*, 1694–1700. (d) Cherest, M.; Felkin, H.; Prudent, N. *Tetrahedron Lett.* **1968**, 2199–2204.
- (58) Alabugin, I. V.; Gilmore, K. M.; Peterson, P. W. *Wiley Interdiscip. Rev.: Comput. Mol. Sci.* **2011**, *1*, 109–141.
- (59) Allinger, N. L.; Riew, C. K. *Tetrahedron Lett.* **1966**, 1269–1272.
- (60) Klunder, A. J. H.; Volkers, A. A.; Zwanenburg, B. *Tetrahedron* **2009**, *65*, 2356–2363.
- (61) Bürgi, H. B.; Dunitz, J. D.; Lehn, J. M.; Wipff, G. *Tetrahedron* **1974**, *30*, 1563–1572.